06

Structure and phase composition of films synthesized by laser sintering from polyvinylidene fluoride of various grades

© E.Yu. Tarasova[1], I.I. Zhuravleva[2], I.A. Bakulin[1], S.I. Kuznetsov[1], A.S. Panin[1,¶]

[1] Lebedev Physical Institute, Samara Branch, Russian Academy of Sciences, Samara, Russia
[2] Samara National Research University, Samara, Russia
¶ E-mail: anton@fian.smr.ru

Received June 9, 2021
Revised August 18, 2021
Accepted August 19, 2021

The processes of laser synthesis of films with a thickness of 80−230 μm from polyvinylidene fluoride of various grades are studied. It is established that the range of synthesis modes does not depend on the grades of PVDF. The content of the piezo active β-phase decreases after laser treatment, but the complete transformation of $\beta \rightarrow \alpha$ does not occur. The process of thermos-oxidative degradation after laser treatment is not observed. Under the same treatment conditions, the higher the open porosity coefficient, the lower the polymer melt flow index (MFI). Depending on the MFI of the initial polymer, the selection of laser exposure modes can control the porosity of the films in the range of 26−68%.

Keywords: laser treatment, polyvinylidene fluoride (PVDF), porous films, melt flow index.

DOI: 10.21883/TPL.2022.15.53811.18913

Polyvinylidene fluoride (PVDF) is fluorine-containing polymer with high piezoelectric and pyroelectric characteristics, nonlinear optical susceptibility, unusually high permittivity for a polymer, chemical resistance to most organic and inorganic solvents, and biocompatibility [{]1 }. The properties of PVDF are largely determined by the phase composition, microstructure and degree of crystallinity of the material, which in turn depend on the conditions of its processing [2]. The traditional use of PVDF is the use as a material for the manufacture of piezo- and pyroelectric sensors. The chemical resistance and biocompatibility of PVDF make it possible to use it as a material for membranes, vascular implants, coatings for bone implants that stimulate tissue regeneration due to the piezoelectric effect, in cell biology and tissue engineering [3–9], and these applications require the production of free, porous PVDF films not attached to the substrate.

At present, the main methods for producing films based on PVDF and its copolymers are melt extrusion or pouring from solutions. To increase the roughness and porosity of the „smooth“ films obtained by such methods, it is necessary to apply additional operations [10]. In the work [11], the method for producing highly porous PVDF films by laser treatment of compressed powders is proposed. The possibility of controlling the porosity of films by changing the parameters of laser exposure and compression pressure is shown. However, for the practical application of this method, it is necessary to establish the main regularities and features of laser sintering of industrially produced grades of PVDF with different characteristics. The purpose of this work is to study the structural-phase transformations of the polymer and the structural features of films obtained from PVDF-2M of various grades by selective laser sintering by radiation with wavelength of 10.6 μm.

Three grades of PVDF-2M were used in the work: A, V and G (according to the classification of the manufacturer „HaloPolymer“), JSC, which are fine powders with a particle size of 15−50 μm. The used materials of grades A, V, G differ somewhat in the melt flow index (MFI): 3.0−7.0, 4.0−7.0, 7.0−20.0 g/10 min, respectively , and have the melting point of 160−165°C. Before laser processing, the polymer was homogenized for 3 h on the mechanical shaking machine, after which it was compacted by pressing on the manual hydraulic press at room temperature under pressure of 5 MPa. Density of the pressed plate of initial powder $\rho = 1.44$ g/cm^3, total porosity 17% (density of initial PVDF 1.75 g/cm^3), thickness 0.7 mm. The samples were sintered using continuous wave CO_2 laser radiation (wavelength 10.6 μm): radiation power $P = 15-34$ W, scanning speed $v = 8-667$ mm/s, laser spot diameter $a = 7$ mm. The power density q of laser radiation and the exposure time $\tau = a/v$ were used as the main characteristics of the laser processing process. The overlap of parallel laser passes was $0.1a$. As a result of laser heating, melting and sintering of powder particles occurred. In this case, the porous PVDF film was formed, the thickness of which depended mainly on the depth of heat of the plate to the melting temperature. The maximum processing speed at given power density was determined by the possibility of separating the film from the pressed material without mechanical defects (tears or breaks), the minimum one by visually noticeable destruction of PVDF (slight charring of the surface).

Density per unit volume and open porosity were determined by the liquid saturation method [12]. Saturation of the samples was carried out in the sealed container at

Table 1. Open porosity factor and density for PVDF films of various grades depending on the laser processing mode

q, W/cm^2	τ, s	K_p, %			ρ, g/cm^3		
		A	V	G	A	V	G
88	0.022	52 ± 2	49 ± 4	48 ± 6	0.9 ± 0.1	0.92 ± 0.07	0.9 ± 0.1
	0.035	46 ± 6	44 ± 5	40 ± 5	1.4 ± 0.1	1.3 ± 0.1	1.1 ± 0.2
78	0.022	52 ± 4	53 ± 2	57 ± 2	0.82 ± 0.04	0.86 ± 0.07	0.8 ± 0.2
	0.042	41 ± 9	37 ± 1	30 ± 3	1.02 ± 0.07	1.12 ± 0.08	1.3 ± 0.1
68	0.021	62 ± 3	68 ± 1	68 ± 5	0.70 ± 0.05	0.60 ± 0.07	0.58 ± 0.09
	0.053	41 ± 4	38 ± 4	26 ± 7	1.1 ± 0.2	1.1 ± 0.1	1.3 ± 0.2

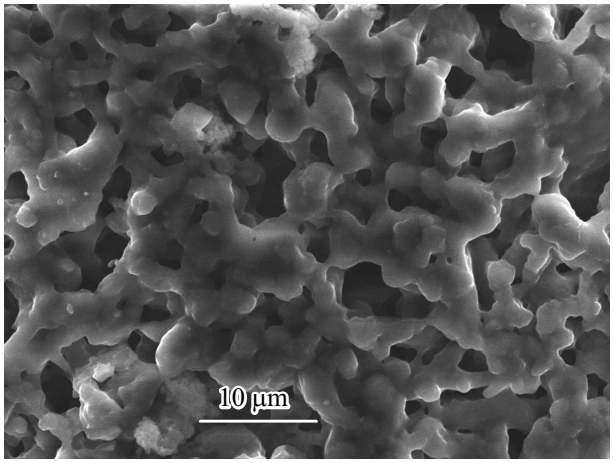

Figure 1. Image of the surface of a PVDF-2M film sintered by laser radiation obtained by scanning electron microscopy. Grade B, $K_p \approx 50\%$.

residual air pressure of 1 Pa, aviation kerosene was used as the working fluid. The structure and phase composition of PVDF-2M were studied by X-ray diffraction and X-ray phase analysis on DRON-3M diffractometer according to the standard procedure. The electron microscopic images of the film surfaces were obtained on JEOL JSM-6390A scanning microscope.

For all three grades of PVDF-2M, the processing modes q and τ practically coincide. The thickness of the films is the same for all grades of PVDF and varies within $80-230\,\mu$m depending on the power density and the laser radiation exposure time. The open porosity and bulk density of the sintered films differ significantly from the porosity and density of the initial half-way product (Table 1). The characteristic surface structure of sintered films is shown in Fig. 1.

The process of laser sintering proceeds due to the softening and/or melting of the polymer, and depending on the mode of laser exposure, both complete remelting and melting of powder particles and their sticking can occur. During laser processing, two competing processes can take place: the increase in open porosity due to thermal-oxidative destruction, rapid heating and expansion of air in the pressed half-way product, or „healing“ pores with melted polymer. It can be seen from Table 1 that K_p decreases with increasing in both power density and exposure time, which is explained by the „healing“ pore process. At the same time, the open porosity for the polymer of grade G, which has a higher MFI, is naturally lower than for PVDF grades A and B. However, the contraction of the polymer also takes place, since the increase up to 1.83 g/cm^3 of the density of the polymer skeleton frame of the porous film (i.e. mineralogical density) is observed, which practically does not depend on the laser exposure mode and is the same for all three grades of polymer.

Laser processing also leads to changes in the crystal structure of the polymer. The initial powders have the same phase composition and microstructure. The diffraction patterns, which completely coincide when superimposed, contain α- and β-phase lines of PVDF and the wide halo in the region of small angles (maximum at $2\theta \sim 9.5^\circ$), which can be caused by diffraction on nanopores or other elements of the polymer microstructure. After laser processing, the structural-phase transformations for grades A and B proceed similarly (Fig. 2); for grade G there are small differences (Fig. 3). The slope angle of the background line (dashed lines in the figures) increases. The rise of the background from the side of small angles can be connected, according to [13], with ultramicroscopic stresses (stresses of the third kind), which lead to the appearance of defects at small distances. The increase in the slope angle of the background line is approximately the same for all three

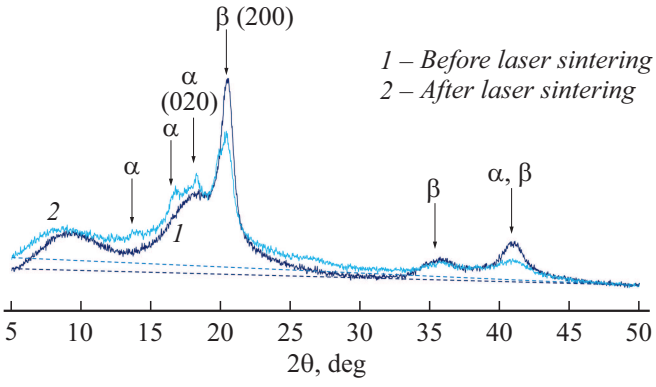

Figure 2. Diffraction patterns of grade A PVDF samples before and after laser processing. $q = 78$ W/cm^2, $\tau = 0.03$ s.

Table 2. Dimensions of coherent scattering regions and spacing of lattice planes for α- and β-phases of PVDF before and after laser processing

Grade PVDF-2M	q, W/cm^2	τ, s	D_α, nm	D_β, nm	d_α, nm	d_β, nm
A	–	–	2.8	6.1	0.485	0.4333
	78	0.03	4.9	6.4	0.4853	0.4403
V	–	–	2.8	6.2	0.4858	0.4332
	78	0.03	4.6	6.2	0.4855	0.4401
G	–	–	2.8	6.1	0.4853	0.4333
	78	0.03	3.8	6.0	0.4855	0.4351

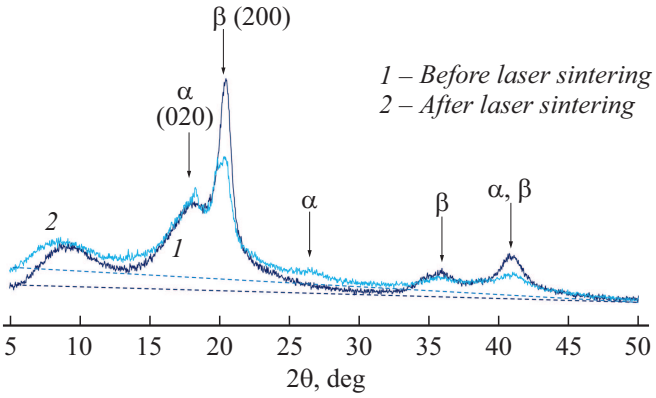

Figure 3. Diffraction patterns of grade G PVDF samples before and after laser processing. $q = 78$ W/cm^2, $\tau = 0.03$ s.

grades of PVDF. The relative intensity of the α-phase lines increases, while the β-phase lines decrease, but the complete $\beta \rightarrow \alpha$ phase transformation does not occur. The shape of the α-phase diffraction lines also changes: they become more bell-shaped, the peak tops become sharper, and the tails broaden. The change in the line shape is associated with the increase in the dispersion of the size distribution of coherent scattering regions (CSRs) and the change in the average CSR size. The shape of peaks of β-phase almost does not change. The results of determining sizes of the CSRs and interplane distances for the most intense diffraction lines α-phase (020) and β–phase (200) are given in Table 2, where D_α, D_β and d_α, d_β are the dimensions of the CSRs and the interplanar distances of the α- and β-phases, respectively.

It can be seen from Table 2 that the average CSR size of the α-phase after laser treatment increases the more, the smaller the MFI of the polymer. The CSR size of the β phase remains virtually unchanged. In this case, the angular positions of the α-phase lines practically do not change for all three grades of PVDF, while the β-phase lines for grades A and B are noticeably shifted towards small angles. It can be assumed that fast laser heating leads to partial melting of the polymer, spreading of the melt, followed by its crystallization into α-phases, and, accordingly, to decrease in the amount of β-phase. As a result of change in the phase composition, structural stresses arise in the material (microstresses and ultramicroscopic stresses i.e. stresses of the second and third kind). Different MFIs of grades A, V and G lead to differences in the spreading of the melt and the magnitude of internal structural stresses and, as a consequence, to different CSRs sizes and spacings of lattice planes of the α- and β-phases.

To estimate the probability of structuring processes, as a result of which infusible three-dimensional addition compounds are formed under the action of laser radiation, the content of sol- and gel-fractions in sintered samples was determined by the extraction method on Soxhlet apparatuses. The extraction results showed that for all three grades of PVDF, the processes of intermolecular dehydrofluorination of the polymer are insignificant under all laser processing modes. The maximum values of the content of the gel-fraction for grade A were 1.2%, for grade B — 1.5%, for grade G — 2.5%.

Thus, the studies performed have shown the possibility of preparing polymer films up to 230 μm thick from PVDF of various grades by laser sintering with a minimum probability of structuring processes. The range of sintering modes and film thickness at the same processing parameters do not depend on the grade of PVDF. After laser processing, the content of the piezoactive β phase decreases, but the complete transformation of $\beta \rightarrow \alpha$ does not occur. The CSR size of the α-phase increases the more, the lower the melt flow index. Under the same processing conditions, the coefficient of open porosity is the higher, the lower the MFI of the polymer. Depending on the MFI of the initial polymer, the porosity of the obtained film can be controlled within the range of 26−68% by selecting the modes of laser exposure.

Funding

Work is performed by the support of the Provincial grant in the field of science and technology for the first half of 2021 of the Government of the Samara region.

Conflict of interest

The authors declare that they have no conflict of interest.

References

[1] M.P. Silva, V. Sencadas, G. Botelho, A.V. Machado, A.G. Rolo, J.G. Rocha, S. Lanceros-Mendez, Mater. Chem. Phys., **122**, 87 (2010). DOI: 10.1016/j.matchemphys.2010.02.067
[2] V. Sencadas, R. Gregorio, Jr., S. Lanceros-Méndez, J. Macromol. Sci. Phys., **48** (3), 514 (2009). DOI: 10.1080/00222340902837527
[3] M. Ulbricht, Polymer, **47** (7), 2217 (2006). DOI: 10.1016/j.polymer.2006.01.084
[4] A. Gugliuzza, E. Drioli, J. Membr. Sci., **446**, 350 (2013). DOI: 10.1016/j.memsci.2013.07.014
[5] P. Hitscherich, S. Wu, R. Gordan, L.-H. Xie, T. Arinze, E.J. Le, Biotechnol. Bioeng., **113** (7), 1577 (2016). DOI: 10.1002/bit.25918
[6] N. Royo-Gascon, M. Wininger, J.I. Scheinbeim, B.L. Firestein, W. Craelius, Ann. Biomed. Eng., **41** (1), 112 (2013). DOI: 10.1007/s10439-012-0628-y
[7] B. Tandon, J.J. Blaker, S.H. Cartmell, Acta Biomater., **73**, 1 (2018). DOI: 10.1016/j.actbio.2018.04.026
[8] A.H. Rajabi, M. Jaffe, T.L. Arinzeh, Acta Biomater., **24**, 12 (2015). DOI: 10.1016/j.actbio.2015.07.010
[9] E.N. Bolbasov, V.L. Kudryavtseva, K.S. Stankevich, L.V. Antonova, V.G. Matveeva, S.T. Tverdokhlebov, V.M. Buznik, Polymeric materials and technologies, **2** (4), 30 (2016).
[10] G.K. Elyashevich, I.S. Kuryndin, E.Yu. Rozova, N.N. Saprykina, Phys. Solid State, **62** (3), 494 (2020). DOI: 10.21883/FTT.2020.03.49018.623
A.I. Ibragimova, I.I. Zhuravleva, S.I. Kuznetsov, A.S. Panin, E.Yu. Tarasova, Kratkiye soobshcheniya po fizike FIAN, **46** (4), 14 (2019) (in Russian) DOI: 10.3103/S1068335619040031
[12] *Rocks. Method for determination of open porosity coefficient by fluid saturation*/ GOST 26450.1–85 (Publishing house of standards, M., 1985).
[13] M.A. Krivoglaz, *Difraktsiya rentgenovskikh luchey i neytronov v neideal'nykh kristallakh* (Nauk. dumka, Kiyev, 1983) (in Russian)